Simultaneous Tether Extraction from Endothelial Cells and Leukocytes: Observation, Mechanics, and Significance

Gaurav Girdhar and Jin-Yu Shao
Department of Biomedical Engineering, Washington University, Saint Louis, Missouri

ABSTRACT It has been hypothesized, from earlier studies on single-tether extraction from individual leukocytes and human umbilical vein endothelial cells, that during rolling of leukocytes on the endothelium, simultaneous extraction of membrane nanotubes (tethers) occurs, resulting in enhancement of the force decrease on the adhesive bond. In this study, using the micropipette aspiration technique and fluorescence microscopy, we show that tethers are indeed extracted simultaneously when an endothelial cell and a leukocyte are separated after brief contact and adhesion, and the endothelial cell contributes much more to the composite tether length. In addition, the constitutive relationship for simultaneous tether extraction is determined with neutrophils and T-lymphocytes as force transducers, and cytokine-stimulated human umbilical vein and dermal microvascular endothelial cells as substrates, respectively. This relationship is consistent with that derived theoretically from the constitutive equations for single-tether extraction from either cell alone. Moreover, we show that simultaneous tether extraction was likely terminated by receptor-ligand bond dissociation. With a biomechanical model of leukocyte rolling, we predict the force history of the adhesive receptor-ligand bond and show that it is remarkably similar for different leukocyte-endothelial cell pairs. Simultaneous tether extraction therefore represents a generic mechanism for stabilizing leukocyte rolling on the endothelium.

INTRODUCTION

Leukocytes roll on the endothelium before extravasation to sites of injury or infection. During the rolling process, adhesive bonds are formed and broken rapidly between selectins and their ligands, whose binding kinetics has been well characterized by several biophysical techniques. However, rapid kinetics alone cannot sufficiently explain the rolling velocity trend observed in flow-chamber experiments, where leukocytes have been shown to roll more stably on ligand-coated substrates than rigid microspheres (1–3). These studies emphasize that the mechanical properties of rolling cells may explain the lesser variance in rolling velocities and longer bond lifetimes observed for cells relative to microspheres. These observations have motivated studies of mechanical properties of individual cellular features such as the extensibility of microvilli (4,5) on leukocytes, membrane tether extraction from endothelial cells (ECs) and leukocytes (6–8), and deformability of interacting cells at high shear stresses (9).

If a pulling force exerted on a leukocyte or endothelial cell surface is large enough, the cell membrane will flow into a cylindrical tube tens of nanometers in diameter (a membrane tether). For pulling rates of <40 μm/s, tether flow can be characterized as a Newtonian process by an effective viscosity (a net energy dissipation term accounting for the membrane flow, the interbilayer slip, and the slip between the membrane and cytoskeleton). This well-characterized relationship can be written as (10)

$$F = F_0 + 2\pi\eta_{\text{eff}}U_t, \tag{1}$$

where F_0 is the threshold force for tether extraction, η_{eff} is the effective viscosity, and U_t is the tether flow velocity. Recent studies on tether extraction from human neutrophils have explored a wider and more physiological range of extraction rates ($0.4 < U_t < 150$ μm/s), indicating a weak power-law relationship between the effective viscosity and tether extraction rate (11). Although the proposed Maxwell-like model demonstrated aptly the shear thinning effect of high tether extraction rates on the effective viscosity, the more concise Newtonian model (Eq. 1) is sufficient to characterize tether extraction in the current range of pulling rates ($0.5 < U_t < 20$ μm/s). Using Eq. 1, the constitutive equation for simultaneous tether extraction (one tether each from leukocytes and endothelial cells, with the receptor-ligand bond in the middle) can be derived from individual constitutive equations used to describe single-tether extraction from either cell. Furthermore, this way of deriving the constitutive equation for simultaneous tether extraction from two interacting identities can be used to predict the constitutive parameters for simultaneous tether extraction during secondary capture of leukocytes from the circulation onto endothelial cells via previously adhered platelets or leukocytes.

It is apparent that the mechanism governing leukocyte rolling stability involves a substantial decrease in the force imposed on the receptor-ligand bond, facilitating preferred longer bond lifetimes that lead to more stable rolling and eventual arrest of the rolling leukocytes on the inflamed endothelium (5,12). Since the pulling or extensional force

Submitted March 20, 2007, and accepted for publication June 27, 2007.

Address reprint requests to Jin-Yu Shao, PhD, Dept. of Biomedical Engineering, Washington University in St. Louis, Campus Box 1097, Rm. 290E, Whitaker Hall, One Brookings Dr., St. Louis, MO 63130-4899. Tel.: 314-935-7467; Fax: 314-935-7448; E-mail: shao@biomed.wustl.edu.

Editor: Michael Edidin.

0006-3495/07/12/4041/12 $2.00

doi: 10.1529/biophysj.107.109298

experienced by each adhesive bond between the leukocyte and endothelium is ~100–1000 pN in the absence of microvillus extension or tether extraction, it has been hypothesized that tethers are extruded from both interacting cells in the rolling process (7,12). In addition, the endothelial cell has been hypothesized to contribute much more to the composite tether length owing to its three- to fourfold lower effective viscosity. Moreover, multiple occurrences of simultaneous tether extraction would also be highly likely in vivo at higher shear stresses and would be expected to confer increased stability upon the rolling leukocyte. A summary of these possible scenarios is shown in Fig. 1. Out of all these scenarios, single- and double-tether extraction from individual leukocytes and endothelial cells (Fig. 1, *A–D*) have been investigated previously (6–8,12,13). Our recent study on double-tether extraction from endothelial cells showed that the dynamic resistance for extraction of double tethers was increased twofold compared to single-tether extraction (6,7,12). Since sufficient membrane materials have been shown to be locally available for tether extraction from both leukocytes and endothelial cells, it may be expected that double tethers, in addition to single tethers, can be extracted simultaneously from both cells during the rolling process. However, whether both threshold forces can be exceeded to allow simultaneous tether extraction is still unknown, because leukocyte and endothelial cell tethers have slightly different threshold forces and the pulling force will decrease rapidly once a tether is extracted.

To our knowledge, no direct or visual evidence exists for simultaneous tether extraction from leukocytes and endothelial cells under either cytokine-stimulated or noninflamed conditions. Moreover, all tether extraction studies have been conducted by pulling cell membranes with an artificial surface like a bead or a metal tip. Therefore, in this study, we used a leukocyte directly as the force transducer of the micropipette aspiration technique (MAT)—which, to the best of our knowledge, has never been applied to direct cell-cell interaction until this study (13,14)—to examine whether double tethers (Fig. 1 *F*), in addition to single tethers (Fig. 1 *E*), can be extracted simultaneously when two cells come briefly into contact and then are separated. With the aid of fluorescence microscopy and cytochalasin D treatment of neutrophils, we showed, for the first time that we know of, that simultaneous tethers (with the major contribution from the endothelial cell) were indeed extracted. We also obtained the constitutive equations for simultaneous tether extraction with the MAT for two different leukocyte-EC pairs (i.e., neutrophils or T-lymphocytes as force transducers, and human umbilical vein endothelial cells (HUVECs) or neonatal human dermal microvascular endothelial cells (HDMECs-n) as substrates). We compared the constitutive parameters determined experimentally and theoretically, and found good agreement, which further substantiates our conclusion of simultaneous tether extraction from the endothelial cell and leukocyte. These findings represent the first experimental and theoretical confirmation of simultaneous tether extraction and highlight its significance as a generic mechanism for stability adopted by leukocytes rolling on the endothelium.

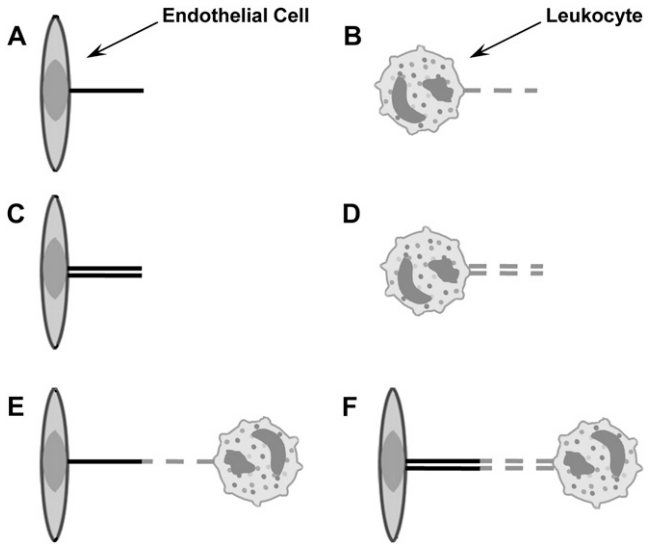

FIGURE 1 Six possible scenarios of tether extraction from endothelial cells and leukocytes in vitro or in vivo. (*A* and *B*) Single-tether extraction from endothelial cells (*A*) or leukocytes (*B*) alone. (*C* and *D*) Double-tether extraction from endothelial cells (*C*) or leukocytes (*D*) alone. (*E* and *F*) Single- (*E*) or double-tether (*F*) extraction from leukocytes and endothelial cells simultaneously.

MATERIALS AND METHODS

Endothelial cell culture and preparation

HUVECs and HDMECs-n were purchased from Cambrex Biosciences (Walkersville, MD) and were cultured in six-well plates or 60-mm petri dishes with endothelial growth medium (EGM-2 for HUVECs and EGM-2MV for HDMECs-n; Cambrex Biosciences). The cells were detached with 5 mM EDTA and cultured on Thermanox coverslips, which were mounted on the side wall of the experimental chamber, as described previously (7). The cultured HUVECs and HDMECs-n were then treated with 10 ng/ml tumor necrosis factor-α (TNF-α; R&D Systems, Minneapolis, MN) for 4 h and 10 ng/ml interleukin 1-β (IL1-β; R&D Systems) for 6 h, respectively.

Three different experimental media were used to conduct tether extraction experiments (Table 1). For neutrophils as force transducers, either a 0.1% human serum albumin (HSA) (Sigma, St. Louis, MO) solution in modified Ca^{2+}/Mg^{2+} free Hanks balanced salt solution (HBSS) (H6648, Sigma) supplemented with 5 mM Mg^{2+}, 0.5 mM EGTA, and 5 μg/ml anti-E-selectin antibody, and buffered with HEPES (Sigma) or a 0.1% HSA solution in HBSS supplemented with Ca^{2+}/Mg^{2+} (HBSS H9269, Sigma) and buffered with HEPES was used. For T-cells as force transducers, a 50% autologous human plasma solution in HBSS supplemented with Ca^{2+}/Mg^{2+} and buffered with HEPES was used in the experimental chamber.

Neutrophil, plasma, and T-cell isolation

The procedure for isolation of human plasma from peripheral blood is outlined in Needham et al. (15). Briefly, 10 ml of citrated peripheral blood sample from healthy volunteers (in accordance with the declaration of Helsinki) was drawn into a sterile tube and centrifuged at 700 $\times$ *g* at 25°C

for 25 min to isolate plasma. Plasma was filtered and stored in cryogenic vials at −20°C for future use.

Neutrophils and T-cells were isolated using a modified finger prick procedure (8,16). Briefly, ~200 μl of blood was collected into a heparinized capillary glass tube (Fisher Scientific, Waltham, MA). The blood was carefully overlaid on 300 μl of gradient solution (mono-poly resolving medium, ICN Biomedicals, Aurora, OH) and the tube centrifuged at 300 × *g* for 15 min. Thereafter, the topmost plasma-and-platelet-rich layer was discarded and the remaining suspension above the red-cell-rich region was collected and mixed with 0.1% HSA solution in HBSS. This cell suspension was centrifuged at 300 × *g* for 5 min to separate neutrophils from the lymphocytes. The resulting supernatant was rich in lymphocytes, whereas the neutrophils were collected at the bottom of the tube in pellet form. Both cell populations were washed with 0.1% HSA solution at 300 × *g* for 5 min before the experiment. The lymphocyte suspension was incubated with 5 μg/ml anti-CD3 FITC antibody for ½ h at 4°C to identify T-cells by fluorescence in the experimental chamber.

Micropipette preparation

Glass micropipettes (~7–8.5 μm in diameter) were prepared with a vertical pipette puller and a microforge, as described elsewhere (16). The narrow opening of the micropipette was filled with either 5% HSA (with neutrophils as force transducers) or 50% autologous plasma (with T-cells as force transducers) and the rest of it was backfilled with HBSS. The micropipette diameter was determined with differential interference contrast microscopy and divided by a correction factor.

Tether extraction and force calculation

Tether extraction was accomplished with the MAT, as described previously (16), but using T-cells and neutrophils directly as force transducers instead of antibody-coated beads. For studying cell-cell interactions, the MAT has the advantage over other techniques in which an artificial surface or bead has to be employed as the force transducer and cells are often affixed to a surface or trapped by laser. With the MAT, one cell is placed inside a glass micropipette and the other is held with a micropipette by a small suction pressure, which ensures little disturbance to the cells.

The experimental schematic for the leukocyte as a force transducer and a surface-attached endothelial cell as substrate is depicted in Fig. 2 *A*. Three specific cases were considered for simultaneous tether extraction from endothelial cells and leukocytes. In the first case, passive neutrophils were used as force transducers and TNF-α-stimulated and attached HUVECs were used as substrates. HBSS supplemented with Ca^{2+}/Mg^{2+} and 0.1% HSA was used as the experimental medium. In the second case, the setup was similar to the first case, except that the experimental medium was replaced by HBSS supplemented with Mg^{2+} (5 mM), EGTA (0.5 mM), and anti-E-selectin antibody (5 μg/ml). In the third case, T-cells were used as force transducers and IL-1β-stimulated and attached HDMECs-n were used as substrates. A 50% solution of autologous plasma in Ca^{2+}/Mg^{2+}-supplemented HBSS was used in this case. All these cases are summarized (Table 1). The Ca^{2+}/Mg^{2+}-supplemented HBSS media were used to engage heterogeneous receptor-ligand pairs when the two cells contacted each other. The Mg^{2+}/EGTA-supplemented HBSS was used to promote LFA-1 into its high-affinity conformation for enhanced binding to ICAM-1 (its ligand on TNF-α-stimulated HUVECs).

The analysis of the tether-extraction experiment was described in detail elsewhere (16). Briefly, the video of interest was transmitted to a Windows computer through a monochrome frame grabber and the region of interest during one adhesion event was tracked with BeadPro8 (a program that has a tracking resolution of ~30 nm and produces the time-displacement data of the force transducer in an ASCII file). Fig. 2 *B* shows a typical curve of the motion-tracking of the leukocyte transducer during a double simultaneous tether event. The initial resistance (after adhesion between the two cells is established and a suction pressure is imposed on the leukocyte) is due to double tethers being extruded simultaneously in parallel (Fig. 2 *B*, region *3*). After one of the two bonds anchoring the tethers is disrupted, the resistance decreases (Fig. 2 *B*, *4*) and only single tethers are extruded simultaneously. The final phase (Fig. 2 *B*, *5*) represents the free unhindered motion of the leukocyte in the micropipette. The tether growth velocities (U_t)—either single-tether (U_{t_1}) or double-tether (U_{t_2})—and the corresponding free-motion velocity of the leukocyte transducer (U_f) were obtained by linear regression. Then the force imposed on the leukocyte transducer (F) can be calculated by (13)

$$F = \pi R_p^2 \Delta p \left(1 - \frac{U_t}{U_f}\right), \tag{2}$$

where Δp is the aspiration pressure inside the left micropipette of radius R_p. The term representing the correction due to the clearance between the transducer and micropipette has been neglected in the above calculation. The reason for this assumption is described below.

The clearance, or gap between the transducer and micropipette, was found to be negligible for cells that fit snugly into the micropipette and offered negligible resistance to motion inside the pipette (two criteria for choice of cellular force transducers). The latter static frictional resistance was inferred from the intercept obtained from a plot of applied suction pressures (Δp) and the corresponding free motion velocity of the cell transducer (U_f) in the micropipette (17), and was found to be negligible for the cell of choice. The slope obtained from the same plot was utilized to calculate the apparent gap between the leukocyte and micropipette. Briefly, the maximum fluid velocity in the pipette was determined by tracking the motion of micron-sized particles or platelets along the centerline under the influence of a known suction pressure. The equivalent length of the micropipette was then calculated by Poiseuille's law (13,17). Next, the dimensionless

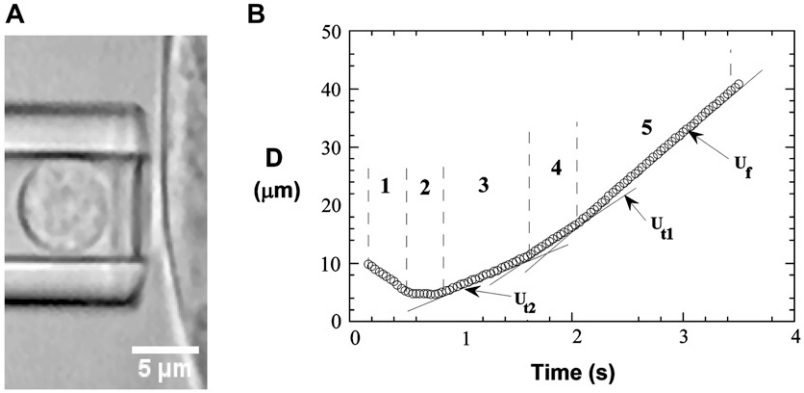

FIGURE 2 The microscopic view of simultaneous tether extraction from leukocytes and attached ECs using MAT. (*A*) The experimental setup for simultaneous tether extraction from a surface-attached endothelial cell (TNF-α-treated HUVEC) and a passive leukocyte (neutrophil) as the force transducer. (*B*) The tracked displacement (D) of a leukocyte during a typical double-tether extraction event: (*1*) Approach toward the EC; (*2*) Contact with the EC; (*3*) Double tether being extracted; (*4*) Single tether being extracted; (*5*) Free motion of the leukocyte. The three fitted solid lines clearly show the distinct velocities during phases 3–5.

apparent gap ($\bar{\varepsilon}$) between the leukocyte and micropipette was calculated using the equation (13,14)

$$\Delta p = \frac{\mu U_f}{R_p}\left[\left(\frac{4\sqrt{2}\pi}{\bar{\varepsilon}^{1/2}} - 32\right) + \frac{8(L_{eq} - D_s)}{R_p}\left(1 - \frac{4}{3}\bar{\varepsilon}\right)\right], \quad (3)$$

where $\Delta p/U_f$ (determined as mentioned above from free motion of neutrophils in the pipette under the influence of a pressure Δp), pipette radius (R_p), equivalent length (L_{eq}, as determined by Poiseuille's law), and cell diameter (D_s, ~4.25 μm for neutrophils and ~3.75 μm for T-lymphocytes) are known. The dimensional gap ($\bar{\varepsilon}R_p$) was determined to be <0.1 μm on average and thus would not significantly affect the force calculation if Eq. 2 was used instead of the equation (13)

$$F = \pi R_p^2 \Delta p\left(1 - \frac{U_t}{U_f}\right)\left(1 - \frac{4\bar{\varepsilon}}{3}\right). \quad (4)$$

The effect of varying clearance (between the force transducer and micropipette) on the calculated force has been discussed previously in detail (14).

Tether extraction from HUVECs and cytochalasin-D-treated neutrophils

HUVECs were detached as described previously (7) and introduced into the experimental chamber with two micropipettes. The smaller micropipette was used to hold the HUVEC under a small suction pressure and the larger micropipette was utilized for the motion of the neutrophil (force transducer) under an applied suction pressure. Neutrophils were isolated from peripheral blood as described previously. The neutrophil cell suspension was then treated with 100 μM cytochalasin D (Sigma) at 37°C for 1 h. Thereafter, the neutrophils were introduced into the experimental chamber and utilized immediately as force transducers to extract simultaneous tethers. The data were recorded on a DVD for later analysis. To confirm the disruption of the actin cytoskeleton upon cytochalasin D treatment, the treated neutrophils were incubated with Alexa Fluor Phalloidin (Molecular Probes, Eugene, OR) and compared with untreated neutrophils labeled with the same dye under similar conditions.

Fluorescent observation of neutrophil-HUVEC simultaneous tethers

Observation of simultaneous tethers was done using two staining procedures: staining HUVECs only, and staining both neutrophils and HUVECs with fluorescent membrane markers. In the first case, TNF-α-stimulated HUVECs were incubated with 5 μg/ml of FM1-43 at 4°C for 45 min and then washed and introduced in the experimental chamber containing passive unlabeled neutrophils. In the latter case, both TNF-α-stimulated HUVECs and neutrophils were incubated with 5 μg/ml of DiO (Molecular Probes) at 4°C for 45 min, washed, and then introduced into the experimental chamber. Tether extraction was carried out either by bringing the two cells into contact and then withdrawing one of the holding micropipettes, or by imposing a suction pressure on the neutrophil (used as a force transducer) after contact with the HUVEC was established.

Statistical analysis

The threshold forces and effective viscosities obtained for the three cases of simultaneous tether extraction were compared within and also to the values obtained for single-tether extraction from cytokine-stimulated and surface-attached endothelial cells. The comparison between intercepts (threshold forces) was conducted using the Tukey test and that between slopes (effective viscosities) was conducted using analysis of variance (18). See Table 2 for a summary of the statistical comparisons done in this study. A significance level of 95% ($p = 0.05$) was chosen for all the tests.

Prediction of force decrease and relative tether lengths

Since the constitutive equations for single and double-tether extraction from endothelial cells and leukocytes were known, it was possible to predict the rate of force decrease and growth of tether length by incorporating the equations into a biomechanical model of leukocyte rolling. We utilized a modified biomechanical model of cell rolling discussed in detail elsewhere (12). The average values of threshold force and effective viscosity for single-tether extraction from HDMECs-n (6) and HUVECs (7) were used in the model. The corresponding parameters for single-tether extraction from neutrophils and T-cells were obtained from previous studies (8,13). The force decrease on the receptor-ligand bond was calculated for four cases: neutrophil-HUVEC simultaneous tether, T-lymphocyte-HDMEC simultaneous tether, neutrophil single tether, and T-lymphocyte single tether. The calculation was repeated for shear rates of 100, 270, and 450 s^{-1} for each of the above cases. An initial composite tether length of 0.35 μm (corresponding to the original length of microvilli), a cell-substrate gap of 0.01 μm, and an optimized time step of 0.1 ms were used for all calculations, and the computations were performed in MATLAB (The Mathworks, Natick, MA) by Euler's method.

RESULTS

Theoretical estimation of threshold force and effective viscosity

The effective viscosity and threshold force for simultaneous tether extraction can be derived from the constitutive relations describing single-tether extraction from either leukocytes or endothelial cells (referred to below as cell 1 and cell 2, respectively). The resultant equation may be used to predict the constitutive parameters for either homotypic (e.g., leukocyte-leukocyte simultaneous tethers in the case of secondary capture) or heterotypic (e.g., endothelial cell-leukocyte or platelet-leukocyte simultaneous tethers in the case of primary or secondary capture, respectively) simultaneous tethers likely to be extracted during the inflammatory response. The equations for single-tether extraction from cell 1 and cell 2 can be written as (Eq. 1):

$$F = F_{0_1} + 2\pi\eta_1 U_1, \quad (5)$$

$$F = F_{0_2} + 2\pi\eta_2 U_2, \quad (6)$$

where F_{0_1} and F_{0_2} are the threshold forces, and η_1 and η_2 are the effective viscosities, for single-tether extraction from cell 1 and cell 2, respectively. The force F represents the force exerted on the receptor-ligand bond between the two cells. The composite tether length of the simultaneous tether is the sum of the individual tether lengths from cell 1 and cell 2. Hence, the rate of change in the simultaneous tether length (tether velocity) is also the sum of the two individual tether velocities,

$$U_t = U_1 + U_2. \quad (7)$$

Combining Eqs. 5–7, we can obtain the following equation for simultaneous tether extraction:

$$F = F_{0_i} + 2\pi\left\{\frac{\eta_1\eta_2}{\eta_1+\eta_2}\right\}U_t, \quad (8)$$

where F_{0_i} is the threshold force for simultaneous tether extraction (F_{0_1} or F_{0_2}, whichever is higher), and the effective viscosity for simultaneous tether extraction is half the harmonic mean of the individual effective viscosities for single-tether extraction from either cell. The theoretical threshold force can also be derived similarly from Eqs. 5–7 as

$$F_0 = \frac{\eta_1 F_{0_2} + \eta_2 F_{0_1}}{\eta_1+\eta_2}. \quad (9)$$

Although F_0 is between F_{0_1} and F_{0_2}, for simultaneous tethers to be extracted, the threshold force would have to be the larger of the individual threshold forces for single-tether extraction from either cell (F_{0_1} and F_{0_2}). F_0 does not represent the true threshold force for simultaneous tether extraction and it only predicts the extrapolated intercept from the experimental correlation between the force and tether-growth velocity for simultaneous tether extraction.

Observation of simultaneous tethers

To confirm the hypothesis that tethers are extracted simultaneously from leukocytes and HUVECs when they are separated after a brief contact and adhesion, the cells were labeled with membrane markers and their fluorescence was observed during tether extraction and retraction. Two specific cases were considered here, as described earlier: HUVECs and neutrophils labeled with DiO, and HUVECs labeled with FM1-43. It should be noted that DiO does not uniformly stain the neutrophil membrane (due to a highly ruffled microvillus-rich surface), and hence, tethers were extracted from the membrane patch with the brightest fluorescence. One frame-by-frame (time lapse of 0.033 s between each frame) observation of simultaneous tether extraction from a neutrophil and a HUVEC labeled with DiO is shown in Fig. 3 *A*. The composite tether (before bond dissociation) and the individual tethers (after bond dissociation in the retraction phase) can be seen within the rectangular region marked in the figure. The topmost panel shows the intact tether just before bond rupture. The middle image (0.033 s later) shows the tether-bond rupture and the start of retraction of the two tethers back to their cells of origin. Notice the slight buckling of the EC tether and rapid retraction immediately after bond rupture. The lower panel (0.066 s later) shows the retraction of the two tethers. Note that the EC tether swings upward, whereas the neutrophil tether retracts almost axially.

Fig. 3 *B* shows two separate snapshots of simultaneous tether extraction from two other HUVEC-neutrophil pairs where only the HUVECs were labeled with FM1-43. The fluorescent tether (the HUVEC contribution to the simultaneous tether) retracted back to the HUVEC after bond rupture (not shown). The approximate position of the neutrophil (force transducer) in the micropipette is marked with a dotted line. In both cases, the contribution to the composite tether was much larger from the HUVEC than from the neutrophil.

To confirm the presence of simultaneous tethers and the relative contribution from each cell to the composite tether, a cytochalasin-D-treated neutrophil was used as the force transducer for the MAT. Exposure of neutrophils to 100 μM cytochalasin D has been shown to reduce the effective viscosity fourfold, which is almost equal to that of HUVECs. Thus, any point force exceeding 50 pN and imposed simultaneously on the neutrophil and the endothelial cell membrane should extrude a composite tether with relatively equal contribution from both cells. To confirm the disruption of actin filaments in neutrophils by cytochalasin D, we labeled the neutrophils with phalloidin after the cytochalasin treatment. The resultant fluorescent images of control and cytochalasin-D-treated neutrophils are shown in Fig. 4 *A*. Neutrophil tethers can be easily visualized upon cytochalasin D treatment, as they are thicker and nonuniform in diameter (J. Y. Shao and J. Xu, unpublished observations), possibly due to a drastic reduction in membrane-cytoskeleton association and loss of elastic energy, contributing to accumulated and easily visualized membrane materials. In contrast, the HUVEC (untreated cell) tether would be expected to be invisible under similar microscopic conditions. As speculated, the neutrophil contribution to the simultaneous tether was clearly visible for the cases shown in Fig. 4 *B* and it is much higher compared to the fluorescence observations shown in Fig. 3 due to an approximately three- to fourfold-reduced effective viscosity. However, this enhanced neutrophil contribution was not observed every time the cells were contacted and separated and it may be attributed to the incomplete disruption of the actin cytoskeleton in the cytochalasin-D-treated neutrophils. The discontinuity of the cortical ring in the cytochalasin-D-treated neutrophil relative to the control (Fig. 4 *A*) suggests only partial disruption of the actin cortex and the observable ''thicker'' tethers may have been extracted only from regions of discontinuity (weakened membrane-cytoskeleton adhesion).

Simultaneous tether extraction from the neutrophil and HUVEC

The MAT was used to extract simultaneous tethers with passive neutrophils as force transducers and TNF-α-treated surface-attached HUVECs as substrates. Two particular cases were considered to engage heterogeneous receptor-ligand pairs on these two cells. In the first case, HBSS with Ca^{2+} (1.2 mM)/Mg^{2+} (0.8 mM) was used as the experimental medium. In the second case, HBSS with Mg^{2+} (5 mM)/EGTA (0.5 mM) supplemented with mouse antihuman E-selectin antibody (5 μg/ml) was used to maximize β_2-dependent interactions since Mg^{2+}/EGTA is known to promote LFA-1 into a high-affinity conformation favoring binding to its major ligand, ICAM-1. If similar constitutive relations are obtained for these two conditions, the conclusion that single and double-tether

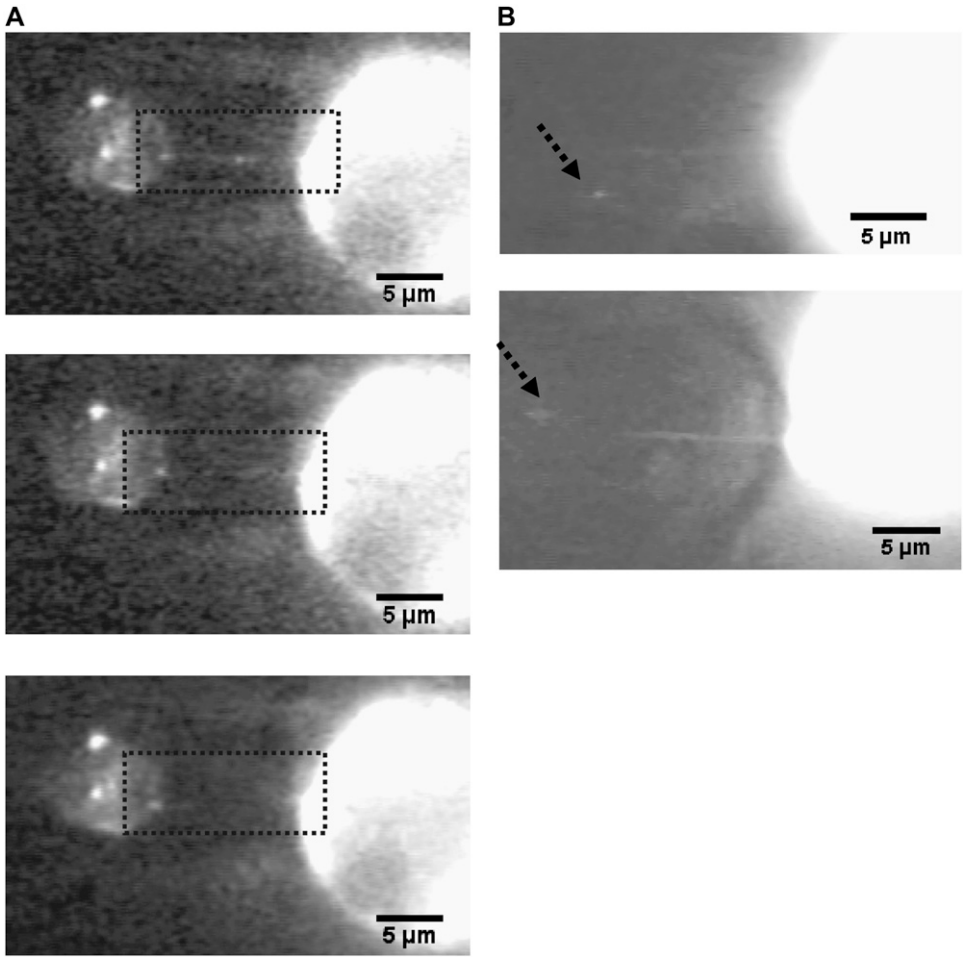

FIGURE 3 (*A*) Simultaneous tether extraction from a neutrophil (*left*) and a HUVEC (*right*), where both cells are labeled with DiO. The three-frame observation for a typical simultaneous tether event (*upper*, elongation; *middle* and *lower*, tether retraction after bond rupture) is shown. The rectangular areas in each frame indicate the region of interest for simultaneous and individual tethers. (*B*) Simultaneous tether extraction from a HUVEC and a neutrophil. The HUVEC, at right, is labeled with FM1-43 and the neutrophil, at left, is unlabeled. The dotted line (*arrowhead*) represents the approximate position of the neutrophil. (Note the larger contribution of the EC to the composite tether length.)

extraction are independent of surface-receptor type, as investigated previously, should also be drawn for simultaneous tether extraction. The results for these two cases are plotted in Fig. 5, *A* and *B*.

Remarkably similar effective viscosity and threshold force are obtained for the two cases from a linear fit to the data. Statistical analysis shows no significant difference between the threshold force and effective viscosity for these two cases and those estimated earlier for single-tether extraction from HUVECs (Table 2). This strengthens the conclusion that the endothelial cell is the major contributor to the total composite tether length and hence to the overall stability of the rolling process. Moreover, the effective viscosity and threshold force obtained from these linear regressions are in excellent agreement with those estimated theoretically using Eq. 8 (Table 3).

Simultaneous tether extraction from T-cells and MECs

Single- and double-tether extraction studies with HUVECs and HDMECs show remarkably similar estimates of threshold force and effective viscosity. Moreover, tether-extraction studies with T-cells and neutrophils also yield similar estimates of the parameters for these two cells. Since the two leukocytes exhibit similar mechanical properties, as also observed for the two endothelial cell lines, the composite tethers from any leukocyte-endothelial combination should yield similar threshold force and effective viscosities. To verify this hypothesis, we extracted tethers with T-cells as force transducers and IL1-β-stimulated HDMECs-n as substrate. The tether force and tether growth velocity correlation is shown in Fig. 5 *C* and is fitted with a linear regression. As shown in Table 2, statistical analysis shows no significant difference for the threshold forces and effective viscosities among the three cases outlined in Table 1 (18). Moreover, similar values are obtained for the effective viscosity from Eq. 8 and from the regression (Table 3).

Simultaneous double-tether extraction from the neutrophil and HUVEC

As hypothesized in Fig. 1 *F*, double tethers were extracted simultaneously from neutrophils and TNF-α stimulated HUVECs in an experimental medium containing Mg^{2+}/EGTA. The duration of contact between the two cells was

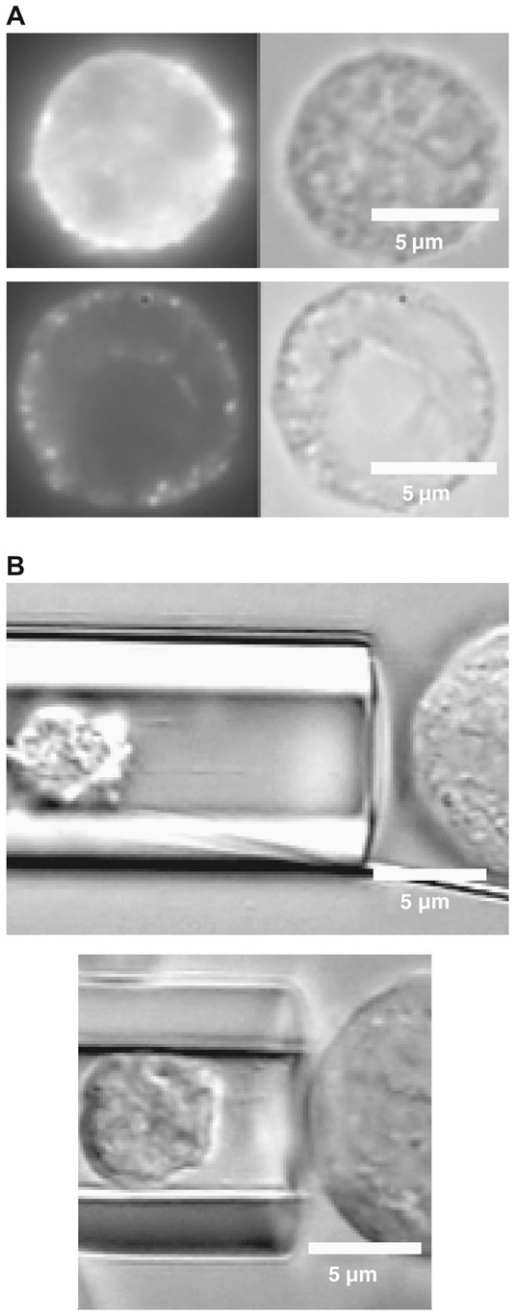

FIGURE 4 (*A*) Disruption of actin filaments in the neutrophil after treatment with 100 μM cytochalasin D. Both control (*upper*) and cytochalasin-treated (*lower*) neutrophils are stained with Phalloidin Alexa Fluor to observe the actin filaments. (*B*) Simultaneous tether extraction from a HUVEC, at right, and a neutrophil treated with 100 μM cytochalasin D, at left. Note the enhanced contribution of the thicker neutrophil tether to the composite tether length and the junction adhesive bond more or less in the middle.

increased to get double-tether events. The force-tether extraction velocity results are plotted in Fig. 5 *D*. The dotted and dashed lines represent double-tether extraction from HUVECs (12) and passive neutrophils (8), respectively. As inferred for the case of simultaneous single-tether extraction, the effective viscosity ($\eta_{eff} = 0.82 \pm 0.22$ pN·s/μm) and threshold force ($F_0 = 99$ pN) agree well with their corresponding theoretically predicted values ($\eta_{eff} = 0.73$ pN·s/μm; $F_0 = 99$ pN) calculated from Eqs. 8 and 9.

Receptor-ligand bond dissociation likely terminates tether flow

Bond lifetimes were measured for the second case (i.e., medium with Mg^{2+}, EGTA, and anti-CD62E antibody) to verify whether simultaneous tether extraction was indeed mediated by the LFA-1-ICAM-1 interaction. The results for the tether force and the logarithm of the corresponding bond lifetime are shown in Fig. 6. An intrinsic bond lifetime of 25 ± 11 s and a reactive compliance of 1.6 ± 0.3 Å were obtained by fitting the force (F) and bond-lifetime ($1/k_{off}$) results with the Levenberg-Marquardt algorithm to the Bell model ($k_{off} = k_{off}^0 e^{\sigma F/k_B T}$) (19), where k_{off}^0 is the reverse rate constant (inverse of the intrinsic bond lifetime), σ is the bond reactive compliance, k_B is the Boltzmann constant and T is the temperature (K). Blocking antibodies to both ICAM-1 and LFA-1 reduced the adhesion frequency dramatically (to ~10% from 30%), confirming the specificity of the interaction. The estimates for the intrinsic off-rate and reactive compliance are within the range of values reported for this interaction by different biophysical techniques (20–22). In conclusion, the kinetic study suggests that tether extraction is probably terminated by LFA-1-ICAM-1 bond dissociation. The termination of tether growth by receptor-ligand (P-selectin-PSGL-1) bond dissociation has also been shown in a previous study (11) and supports the mechanism proposed here.

Force decrease on the receptor-ligand bond

The force decrease on the receptor-ligand bond as a consequence of tether growth was obtained by numerically solving kinematic, force balance, and torque balance equations for a biomechanical model of cell rolling, as developed elsewhere (12). The force history computations done at shear rates of 100, 270, and 450 s^{-1} are shown in Fig. 7, *B* and *D*. At a shear rate of 270 s^{-1}, the instantaneous force on the bond due to a single tether extracted from the neutrophil was ~460 pN, in contrast to ~260 pN for simultaneous extraction of single tethers. A similar trend was observed for the force on the bond due to simultaneous tether extraction from the T-cell and HDMEC-n, and single-tether extraction from the T-cell alone. Thus, the instantaneous force was significantly smaller for both cases of simultaneous tether extraction relative to single-tether extraction from leukocytes and is in accordance with similar trends obtained for the force history for simultaneous double tethers and double tethers from individual cells calculated previously (12). It is obvious that simultaneous tether extraction would facilitate a longer lifetime of the receptor-ligand bond,

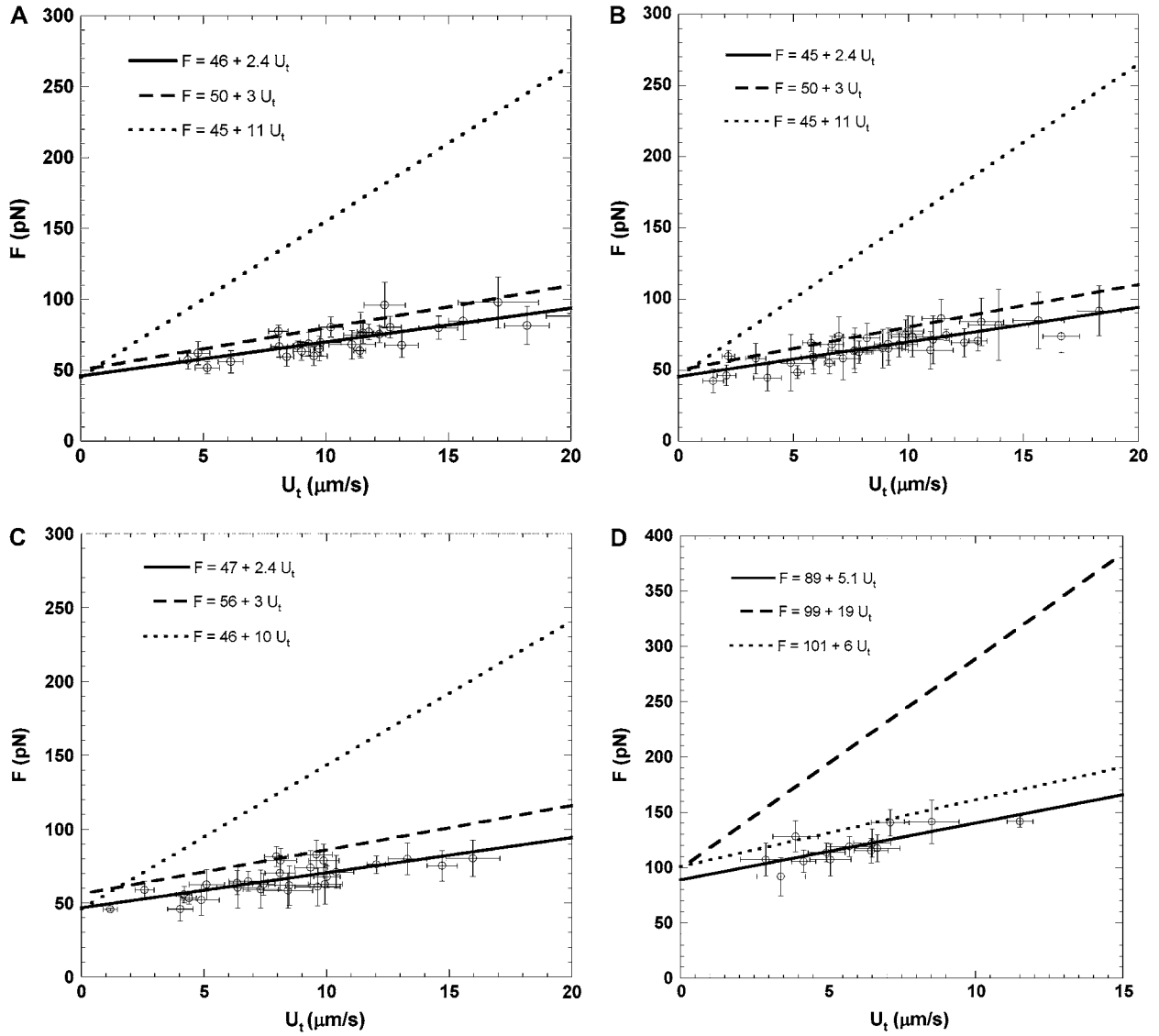

FIGURE 5 Simultaneous single-tether extraction from (*A*) passive neutrophils and TNF-α (10 ng/ml, 4 h) treated surface-attached HUVECs in Ca^{2+}/Mg^{2+} medium, (*B*) passive neutrophils and TNF-α (10 ng/ml, 4 h) treated surface-attached HUVECs in Mg^{2+}/EGTA/anti-E-selectin medium, (*C*) passive T-lymphocytes and surface-attached HDMECs-n treated with IL-1β (10 ng/ml, 6 h) in Ca^{2+}/Mg^{2+} medium, and (*D*) simultaneous double-tether extraction from passive neutrophils and TNF-α (10 ng/ml, 4 h) treated surface-attached HUVECs in Mg^{2+}/EGTA/anti-E-selectin medium. Each point represents an average of 5–20 tethers. The threshold force (intercept) and the effective viscosity (slope/2π) for simultaneous tether extraction can be estimated from the linear regression. In *A* and *B*, the dashed line represents single-tether extraction from attached and TNF-α-stimulated HUVECs and the dotted line represents single-tether extraction from passive neutrophils. In *C*, the dashed line represents single-tether extraction from attached IL-1β-stimulated HDMECs-n and the dotted line represents single-tether extraction from $CD4^+$ T-lymphocytes. In *D*, the dashed line represents double-tether extraction from passive neutrophils and the dotted line represents double-tether extraction from attached TNF-α-stimulated HUVECs.

causing the leukocyte to roll more stably on the endothelium. Moreover, similar force histories for different combinations of leukocyte and endothelial cell support the ubiquity of the force-decrease mechanism during leukocyte rolling. The differential in the growth velocity of the neutrophil and endothelial cell tethers is responsible for the remarkably reduced instantaneous bond force in the case of simultaneous tethers and is illustrated in Fig. 7, *A* and *C*. As expected, the EC contributes more significantly to the composite tether length than the leukocyte in both instances of simultaneous tether extraction.

DISCUSSION

This is the first study that we know of to demonstrate simultaneous tether extraction from leukocytes and endothelial cells and apply the MAT to direct cell-cell interactions. Fluorescent labeling of neutrophils and HUVECs

TABLE 1 Three conditions of simultaneous tether extraction experiments with the MAT

Transducer	Substrate	Media in Chamber
Neutrophil	TNF-α treated HUVECs	Ca^{2+}/Mg^{2+} enriched HSA/HBSS
Neutrophil	TNF-α treated HUVECs	Mg^{2+}/EGTA enriched HSA/HBSS
T-cell	IL1-β treated HDMECs	Ca^{2+}/Mg^{2+} enriched HSA/HBSS

The conditions are based on compositions of the force transducer, substrate, and medium to engage heterogeneous receptor-ligand pairs.

TABLE 3 Summary of the parameter values and their 68% confidence limits for simultaneous tether extraction from passive leukocytes and cytokine-stimulated endothelial cells

Transducer	F_0 (pN)	η_{eff} (pN·s/μm)	R	F_0 (pN)*	η_{eff} (pN·s/μm)*
Attached TNF-α-stimulated HUVECs					
Neutrophil†	46 ± 3	0.39 ± 0.04	0.84	49	0.38
Neutrophil‡	46 ± 4	0.38 ± 0.06	0.80	49	0.38
Attached IL-1β-stimulated HDMECs-n					
T-Cell‡	47 ± 4	0.39 ± 0.06	0.77	53	0.37

*The predicted values for threshold force (F_0; Eq. 9) and effective viscosity (η_{eff} ; Eq. 8) agree well with those determined experimentally.
†Experiments performed in the presence of Mg^{2+}/EGTA.
‡Experiments performed in the presence of Mg^{2+}/Ca^{2+}.

together or of HUVECs only clearly shows the presence of two tethers, with the major contribution emanating from HUVECs. This observation was expected, since the threshold force required for tether extraction from both cells is only slightly different, ~50 pN, and a fourfold difference exists in the effective viscosity, thereby permitting enhanced HUVEC membrane flow during simultaneous tether extraction. The fluorescence observations were also confirmed by observing tethers from cytochalasin-D-treated neutrophils. This treatment has been known to reduce the effective viscosity of neutrophils to the value representative of HUVECs (16). Hence, an almost equal contribution was expected from the neutrophil when tethers are extracted simultaneously from the treated neutrophil and the HUVEC. This is confirmed by the observation shown in Fig. 4 *A*, thereby reinforcing the existence of simultaneous tethers when the two cells are separated after brief contact and adhesion.

One of the objectives of this study was to show that simultaneous tether extraction is an intrinsic membrane protrusion process just like single or double-tether extraction from individual cells alone. Since a spherical force transducer (which provides a snug fit inside the micropipette) is essential to minimize errors associated with the gap in the MAT experiments, the use of a passive leukocyte was mandatory. Thus, the expression of contributing receptor-ligand pairs that represent the link between the two tethers constituting the simultaneous tether was altered by the use of divalent cations and not by treating the neutrophil with interleukins or other chemotactic agents (known to alter the activation state and shape of the cell). In the first case (neutrophils and TNF-α-stimulated HUVECs), HBSS with Ca^{2+} (~1.25 mM) and Mg^{2+} (~0.8 mM) was used as the experimental medium. The majority of the interactions observed were expected to be a combination of CD62E-PSGL-1, CD62E-CD44 (23), and some ICAM-1-β_2-integrin (low-affinity state) interactions (24). In the second case, HBSS with Ca^{2+} and Mg^{2+} was supplemented with 5 mM

TABLE 2 Statistical comparison of the effective viscosities (slope/2π) and threshold forces (intercepts) for three scenarios

Cases*	Cell line(s)†	Force transducers	p (slope)	p (intercept)
A	HDMECs	T-cells; anti-CD54 beads; anti-CD62E beads	0.21	>0.05
B	HUVECs	Neutrophils; anti-CD54 beads; anti-CD62E beads	0.06	>0.05
C	HUVECs HDMECs	Neutrophils (HUVECs); Neutrophils (HUVECs); T-cells (HDMECs)	0.99	>0.05

*Comparisons are between: (A) single tethers, extracted from HDMECs-n with anti-CD54 and anti-CD62E coated beads as transducers, and simultaneous tethers, extracted from T-cell-HDMEC-n with T-cells as transducers; (B) single tethers, extracted from HUVECs with anti-CD54 and anti-CD62E coated beads as transducers, and simultaneous tethers, extracted from neutrophil-HUVEC with neutrophils as transducers; and (C) single tethers extracted simultaneously from either neutrophil-HUVEC or T-cell-HDMECs-n interactions (Table 1). The comparisons were done using analysis of variance (slopes) and Tukey test (intercepts) and the p values for a significance level of 95% were obtained (18).
†The endothelial cell lines are attached and cytokine-stimulated with IL-1β for HDMECs-n and TNF-α for HUVECs.

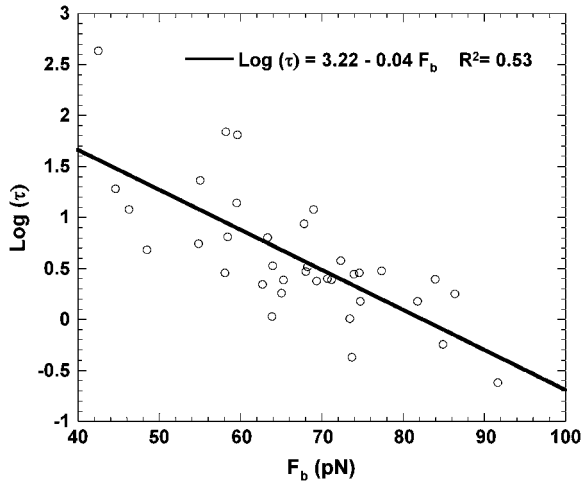

FIGURE 6 The bond lifetime (τ) as a function of pulling force (F_b) for the LFA-1-ICAM-1 interaction. Simultaneous single-tether extraction was accomplished from passive neutrophils treated with Mg^{2+}/EGTA and surface-attached HUVECs stimulated with TNF-α (10 ng/ml, 4 h). Each point is an average of multiple adhesion events. The error bars for each point have been removed for clarity.

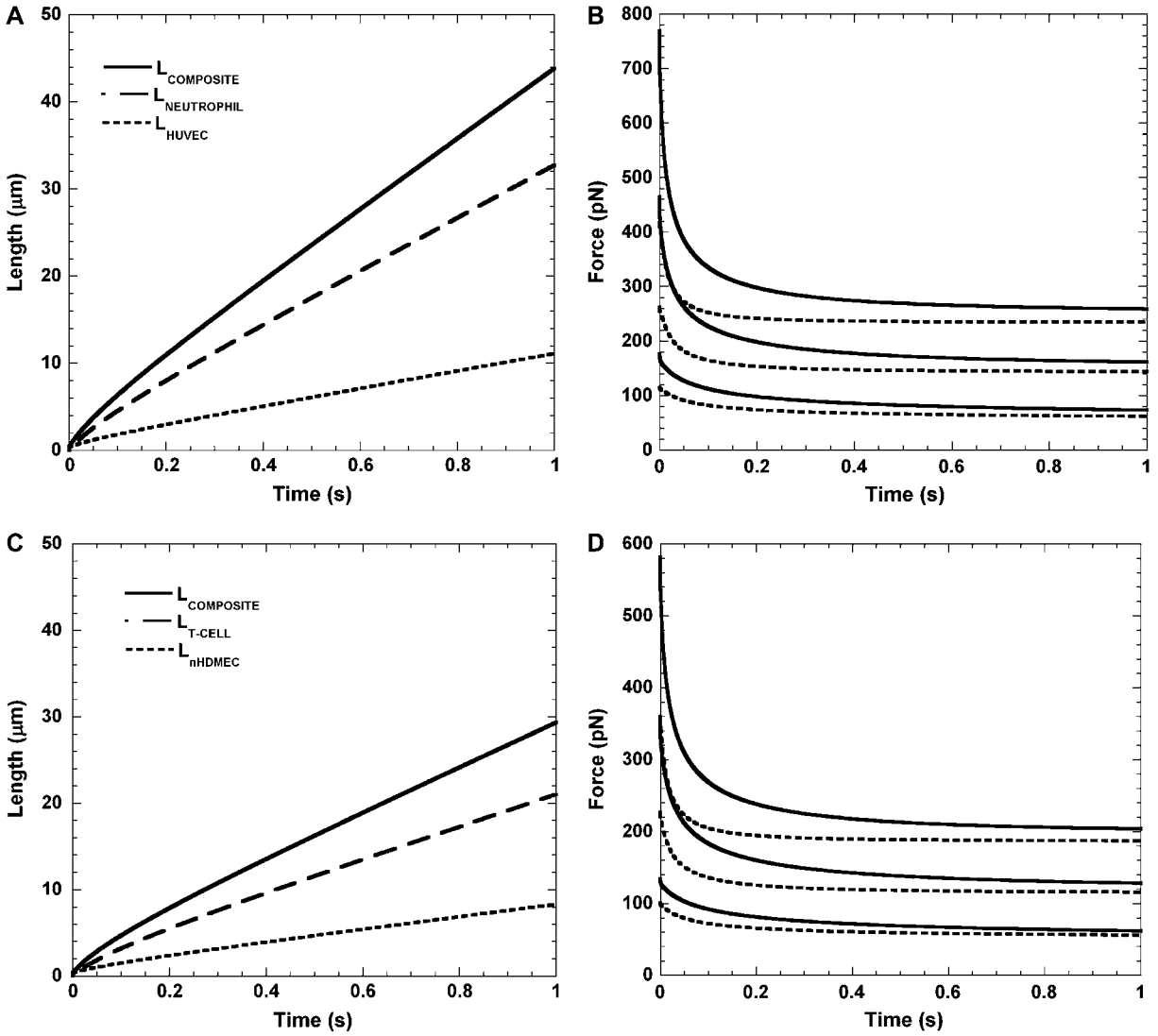

FIGURE 7 Calculated tether lengths and force histories for simultaneous tether extraction from endothelial cells and leukocytes. (*A*) The calculated growth of the simultaneous single HUVEC-neutrophil tether, and the individual contributions from the neutrophil and HUVEC to the total tether length *(solid line)* are plotted for a shear rate of 270 s^{-1}. The *dashed* and *dotted* lines represent the contributions from the neutrophil and HUVEC, respectively. An initial microvillus length of 0.35 μm (L_0) was used in the computation. Note that $L_2 = L_0$ at time 0. (*B*) The calculated decrease in the bond force over time during simultaneous extraction of three single neutrophil-HUVEC tethers is plotted for shear rates of 100, 270, and 450 s^{-1} (*dotted lines, bottom to top*). The solid line represents the calculated force decrease for the case of tether extraction from the neutrophil alone and is plotted here for comparison with the simultaneous tether. (*C*) The calculated growth of the single simultaneous HDMEC-n-T-cell tether and the individual contributions from the T-cell and HDMEC-n to the total tether length *(solid line)* are plotted for a shear rate of 270 s^{-1}. The dashed and dotted lines represent contributions from the T-cell and HDMEC-n, respectively. An initial microvillus length of 0.35 μm (L_0) was used in the computation. Note that $L_2 = L_0$ at time 0. (*D*) The calculated decrease in the bond force over time during simultaneous extraction of three single T-cell-HDMEC-n tethers is plotted for shear rates of 100, 270, and 450 s^{-1} (*dotted lines, bottom to top*). The solid line represents the calculated force decrease for the case of tether extraction from the T-cell alone and is plotted here for comparison with the simultaneous tether.

Mg^{2+} and 0.5 mM EGTA to promote LFA-1 to its high-affinity conformation for sustained interaction with ICAM-1. Since different divalent cation media yield similar values of threshold force and effective viscosity, we can conclude that simultaneous tether extraction is unaffected by the receptor-ligand pair connecting the two tethers.

For a passive neutrophil, ~10,000 β_2 integrins reside in their high-affinity conformation (25), ~1000 of which are Mac-1 (26). Hence, the majority of the interactions reported in the second case considered in this study, where 5 mM Mg^{2+} and 0.5 mM EGTA were used, are due to LFA-1-ICAM-1 binding. This was confirmed by measuring the tether-bond lifetimes and fitting the results with the Bell model, which aptly demonstrates the effect of force on tether-bond lifetime (27). The bond lifetime measurements reported herein represent the dissociation of a single tether

bond, which is the more likely occurrence at adhesion frequencies lower than 20% (although adhesion frequency alone does not govern single bond probabilities), even in the case of clustered receptor-ligand distributions, as shown in our recent study (28). Moreover, an approximate upper limit of the LFA-1 density on a resting neutrophil can be estimated as $50/\mu m^2$ (29). Similarly, the density of ICAM-1 on TNF-α-activated HUVECs can be estimated as $1000/\mu m^2$ (29). Assuming the average tether radius to be 0.1 μm, the number of LFA-1 receptors at the tip of the tether from the neutrophil can be calculated as ~2, and the density of ICAM-1 at the tip of the tether from the HUVEC as ~30. With these distributions, ~95% of the bonds between LFA-1 and ICAM-1 in this study would be probabilistically expected to behave as single tether-bond interactions, irrespective of the bond-cluster size and the range of contact time for bond formation (28). The kinetic parameters obtained in this study were within the range of those determined elsewhere for this receptor-ligand pair using several different biophysical techniques (20–22). This shows that receptor-ligand bond dissociation is the likely mechanism for the termination of tether flow, a conclusion supported by a recent report on a study involving tether extraction from neutrophils (11).

To demonstrate that simultaneous tether extraction is a ubiquitous phenomenon among leukocytes, tethers were extracted using both T-cells and neutrophils as force transducers. T-cells and HDMECs-n were exposed to a condition similar to that in one of the earlier two cases, i.e., HBSS with Ca^{2+} (~1.25 mM) and Mg^{2+} (~0.8 mM). A majority of passive T-cells do not express functional forms of PSGL-1, and thus, interaction of this ligand with endothelial selectins is not likely. However, a few integrins have been implicated in facilitating lymphocyte rolling via $\alpha_4\beta_1$ (on lymphocytes)-VCAM-1 (on inflamed endothelium) interactions in the presence of divalent cations (30). The CD40-CD154 interaction may also contribute to adhesion between T-cell and stimulated HDMEC (31). Recent findings also show the predominance of $CCR8^+$ T-cells in normal human skin, indicating chemokine-specific dermal trafficking mechanisms (32). It should, however, be noted that the objective here was not to determine individual receptor-ligand pairs anchoring the simultaneous tethers but merely to engage a heterogeneous population from which to extract the tethers. Simultaneous tether extraction from HUVECs and neutrophils was found, statistically, to be mechanically the same as that from T-cells and HDMECs-n, (Table 3), supporting the similarity in mechanical properties of different passive circulating leukocytes and activated endothelial cells (of various lineage), as investigated in early and more recent individual-tether-extraction studies (6,8,12). Moreover, the effective viscosities estimated from the MAT experiments are in excellent agreement with those calculated theoretically applying Eq. 8. This validates the utility of the theoretical simultaneous tether relation for estimating effective viscosities for other possible interacting pairs under different conditions.

A mechanism for stabilizing leukocyte rolling on the endothelium that is based on the force decrease due to tether extraction has been proposed previously (5,7) and also discussed in detail elsewhere (12). More detailed models of leukocyte tethering on ligand-coated substrates (33,34) and endothelial cells (34) also predict the force drop on the receptor-ligand bond after tether extraction, and estimate the corresponding decrease in apparent bond-dissociation constants for receptor-ligand interactions. A higher relative contribution from the endothelial cell to the composite tether length was predicted in the calculations presented here and was shown to account for the reduced instantaneous force on the receptor-ligand bond thereby expected to promote enhanced leukocyte stabilization. The calculated results for the enhanced EC contribution to the simultaneous tether strongly reinforce our fluorescence and tether constitutive equation results. Thus, similar mechanisms of stabilization may be expected for other combinations of leukocyte-endothelial tethers.

Of the cases proposed earlier in this article, and during the early leukocyte rolling phase, simultaneous extraction of tethers when a passive leukocyte and EC are brought into contact seems to be the most likely occurrence (Fig. 1 *E*). This is supported by the slightly lower overall effective viscosity obtained from the tether-force and tether-velocity correlations. The results suggest that a point force imposed simultaneously on both cell membranes via apposed receptor-ligand pairs is sufficiently high to ensure membrane flow from both cells, even though the force drops dramatically after tether formation is initiated from either one of the cells. Although the exact timescale of simultaneous tether extraction is unknown, it is evident that membrane flow initiation from both cells occurs before the instantaneous tether force falls below the threshold force for tether extraction from either cell. Our recent comprehensive modeling study of force history during leukocyte rolling on the endothelium shows the stabilizing effect of simultaneous tethers to be most predominant within the physiological shear rate range of 200–500 s^{-1} (33). Within this range, the pulling force is larger than the individual threshold forces for simultaneous tether extraction and also permits sufficiently longer initial bond lifetimes for stable rolling. It should be noted, however, that the selectivity of occurrence of individual cases proposed earlier (Fig. 1) may be strongly influenced by dynamic force-loading rates, leukocyte activation, receptor-ligand densities, and their distributions on apposed cell surfaces, besides other factors. These factors and their influence on rolling stabilization remain to be investigated in the future.

CONCLUDING REMARKS

This study conclusively shows that simultaneous tethers are indeed extracted when a leukocyte and an endothelial cell are separated after brief contact and adhesion. The enhanced contribution of the endothelial cell to the composite tether predicted by the biomechanical model of leukocyte rolling is

confirmed by fluorescence and cytochalasin D experiments. Moreover, the agreement between the theoretically predicted values and those obtained with the MAT experiments strongly reinforces the concept of simultaneous tether extraction from endothelial cells and leukocytes. However, the tether growth velocity, and thus the expected stabilization, may strongly depend on the applied force history, a subject to be addressed in future investigations.

This work was supported by the National Heart, Lung and Blood Institute (R01 HL069947).

REFERENCES

1. Park, E. Y., M. J. Smith, E. S. Stropp, K. R. Snapp, J. A. DiVietro, W. F. Walker, D. W. Schmidtke, S. L. Diamond, and M. B. Lawrence. 2002. Comparison of PSGL-1 microbead and neutrophil rolling: microvillus elongation stabilizes P-selectin bond clusters. *Biophys. J.* 82:1835–1847.
2. Ramachandran, V., M. Williams, T. Yago, D. W. Schmidtke, and R. P. McEver. 2004. Dynamic alterations of membrane tethers stabilize leukocyte rolling on P-selectin. *Proc. Natl. Acad. Sci. USA.* 101:13519–13524.
3. Yago, T., A. Leppanen, H. Qiu, W. D. Marcus, M. U. Nollert, C. Zhu, R. D. Cummings, and R. P. McEver. 2002. Distinct molecular and cellular contributions to stabilizing selectin-mediated rolling under flow. *J. Cell Biol.* 158:787–799.
4. Evans, E., V. Heinrich, A. Leung, and K. Kinoshita. 2005. Nano- to microscale dynamics of p-selectin detachment from leukocyte interfaces. I. Membrane separation from the cytoskeleton. *Biophys. J.* 88:2288–2298.
5. Shao, J.-Y., H. P. Ting-Beall, and R. M. Hochmuth. 1998. Static and dynamic lengths of neutrophil microvilli. *Proc. Natl. Acad. Sci. USA.* 95:6797–6802.
6. Chen, Y., G. Girdhar, and J. Y. Shao. 2007. Single membrane tether extraction from adult and neonatal dermal microvascular endothelial cells. *Am. J. Physiol. Cell Physiol.* 292:C1272–C1279.
7. Girdhar, G., and J. Y. Shao. 2004. Membrane tether extraction from human umbilical vein endothelial cells and its implication in leukocyte rolling. *Biophys. J.* 87:3561–3568.
8. Xu, G., and J. Y. Shao. 2005. Double tether extraction from human neutrophils and its comparison with CD4+ T-lymphocytes. *Biophys. J.* 88:661–669.
9. Jadhav, S., C. D. Eggleton, and K. A. Konstantopoulos. 2005. 3-D computational model predicts that cell deformation affects selectin-mediated leukocyte rolling. *Biophys. J.* 88:96–104.
10. Hochmuth, R. M., J. Y. Shao, J. Dai, and M. P. Sheetz. 1996. Deformation and flow of membrane into tethers extracted from neuronal growth cones. *Biophys. J.* 70:358–369.
11. Heinrich, V., A. Leung, and E. Evans. 2005. Nano- to microscale dynamics of P-selectin detachment from leukocyte interfaces. II. Tether flow terminated by P-selectin dissociation from PSGL-1. *Biophys. J.* 88:2299–2308.
12. Girdhar, G., Y. Chen, and J. Y. Shao. 2007. Double-tether extraction from human umbilical vein and dermal microvascular endothelial cells. *Biophys. J.* 92:1035–1045.
13. Shao, J.-Y., and R. M. Hochmuth. 1996. Micropipette suction for measuring piconewton forces of adhesion and tether formation from neutrophil membranes. *Biophys. J.* 71:2892–2901.
14. Shao, J.-Y., G. Xu, and P. Guo. 2004. Quantifying cell-adhesion strength with micropipette manipulation: principle and application. *Front. Biosci.* 9:2183–2191.
15. Needham, D., M. Armstrong, D. L. Hatchell, and R. S. Nunn. 1989. Rapid deformation of ''passive'' polymorphonuclear leukocytes: the effects of pentoxifylline. *J. Cell. Physiol.* 140:549–557.
16. Shao, J.-Y., and J. Xu. 2002. A modified micropipette aspiration technique and its application to tether formation from human neutrophils. *J. Biomech. Eng.* 124:388–396.
17. Shao, J.-Y., and R. M. Hochmuth. 1997. The resistance to flow of individual human neutrophils in glass capillary tubes with diameters between 4.65 and 7.75 μm. *Microcirculation* 4:61–74.
18. Zar, J. H. Biostatistical Analysis. 1999. Prentice Hall, Upper Saddle River, N.J.
19. Bell, G. I. 1978. Models for the specific adhesion of cells to cells. *Science.* 200:618–627.
20. Labadia, M. E., D. D. Jeanfavre, G. O. Caviness, and M. M. Morelock. 1998. Molecular regulation of the interaction between leukocyte function-associated antigen-1 and soluble ICAM-1 by divalent metal cations. *J. Immunol.* 161:836–842.
21. Sarantos, M. R., S. Raychaudhuri, A. F. Lum, D. E. Staunton, and S. I. Simon. 2005. LFA-1 mediated adhesion stability is dynamically regulated through affinity and valency during bond formation with ICAM-1. *J. Biol. Chem.* 280:28290–28298.
22. Zhang, X., E. Wojcikiewicz, and V. T. Moy. 2002. Force spectroscopy of the leukocyte function-associated antigen-1/intercellular adhesion molecule-1 interaction. *Biophys. J.* 83:2270–2279.
23. Katayama, Y., A. Hidalgo, J. Chang, A. Peired, and P. S. Frenette. 2005. CD44 is a physiological E-selectin ligand on neutrophils. *J. Exp. Med.* 201:1183–1189.
24. Takagi, J., B. M. Petre, T. Walz, and T. A. Springer. 2002. Global conformational rearrangements in integrin extracellular domains in outside-in and inside-out signaling. *Cell.* 110:599–611.
25. Lum, A. F. H., C. E. Green, G. R. Lee, D. E. Staunton, and S. I. Simon. 2002. Dynamic regulation of LFA-1 activation and neutrophil arrest on intercellular adhesion molecule 1 (ICAM-1) in shear flow. *J. Biol. Chem.* 277:20660–20670.
26. Diamond, M. S., D. E. Staunton, S. D. Marlin, and T. A. Springer. 1991. Binding of the integrin Mac-1 (CD11b/CD18) to the third immunoglobulin-like domain of ICAM-1 (CD54) and its regulation by glycosylation. *Cell.* 65:961–971.
27. Chen, S., and T. A. Springer. 2001. Selectin receptor-ligand bonds: formation limited by shear rate and dissociation governed by the Bell model. *Proc. Natl. Acad. Sci. USA.* 98:950–955.
28. Shao, J.-Y., and G. Xu. 2007. The adhesion between a microvillus-bearing cell and a ligand-coated substrate: a Monte Carlo study. *Ann. Biomed. Eng.* 35:397–407.
29. Lomakina, E. B., and R. Waugh. 2004. Micromechanical tests of adhesion dynamics between neutrophils and immobilized ICAM-1. *Biophys. J.* 86:1223–1233.
30. De Chateau, M., S. Chen, A. Salas, and T. A. Springer. 2001. Kinetic and mechanical basis of rolling through an integrin and novel Ca^{2+}-dependent rolling and Mg^{2+}-dependent firm adhesion modalities for the $\alpha_4\beta_7$-MAdCAM-1 interaction. *Biochemistry.* 40:13972–13979.
31. Grewal, I. S., and R. A. Flavell. 1998. CD40 and CD154 in cell-mediated immunity. *Annu. Rev. Immunol.* 16:111–135.
32. Schaerli, P., L. Ebert, K. Willimann, A. Blaser, R. S. Roos, P. Loetscher, and B. A. Moser. 2004. Skin-selective homing mechanism for human immune surveillance T Cells. *J. Exp. Med.* 199:1265–1275.
33. King, M. R., V. Heinrich, E. Evans, and D. A. Hammer. 2005. Nano- to microscale dynamics of P-selectin detachment from leukocyte interfaces. III. Numerical simulation of tethering under flow. *Biophys. J.* 88:1676–1683.
34. Yu, Y., and J.-Y. Shao. 2007. Simultaneous tether extraction contributes to neutrophil rolling stabilization: a model study. *Biophys. J.* 92: 418–429.